The kinetics of $L1_0$ superstructure formation in the Cu–56Au alloy (at. %): resistometric study

Polina O. Podgorbunskaya*[1,2], student, laboratory assistant of Strength Laboratory
Dmitry A. Zgibnev[1,2], student, laboratory assistant of Strength Laboratory
Alyona A. Gavrilova[1,2], student, laboratory assistant of Strength Laboratory
Oksana S. Novikova[2,3], PhD (Physics and Mathematics), senior researcher of Strength Laboratory
Aleksey Yu. Volkov[2,4], Doctor of Sciences (Engineering), Head of Strength Laboratory

[1]*Ural Federal University named after the first President of Russia B.N. Yeltsin, Yekaterinburg (Russia)*
[2]*M.N. Mikheev Institute of Metal Physics of Ural Branch of RAS, Yekaterinburg (Russia)*

*E-mail: podgorbunskaua@imp.uran.ru,
   polina.podgorbunskaya@yandex.ru

[3]ORCID: https://orcid.org/0000-0003-0474-8991
[4]ORCID: https://orcid.org/0000-0002-0636-6623

Abstract: Due to the improved strength properties compared to the equiatomic Cu–50 at. % Au alloy, non-stoichiometric Cu–56 at. % Au alloy can be used both in dentistry and as a corrosion-resistant conductor of weak electrical signals in tool engineering. The work studies the kinetics of the disorder→order phase transformation in the Cu–56Au alloy, during which the disordered fcc lattice ($A1$-phase) is rearranged into an atomically ordered one with the $L1_0$ superstructure. The initial disordered state of the alloy was obtained in two ways: applying plastic deformation by 90 % or quenching at a temperature of above 600 °C (i. e., from the region of the $A1$-phase existence). To form the $L1_0$ superstructure, annealing was carried out at temperatures of 200, 225, and 250 °C. The annealing duration ranged from 1 h to 2 months. Resistometry was chosen as the main technique to study the kinetics of the disorder→order transformation. The temperature dependences of the electrical resistivity of the alloy in various structural states are obtained. The authors constructed the graphs of the electrical resistance dependence on the annealing time logarithm, based on which, the rate of the new phase formation was estimated. To evaluate the structural state of the alloy at various transformation stages, the authors used X-ray diffraction analysis (XRD). The crystal structure rearrangement during the transformation is shown by the example of splitting the initial cubic $A1$-phase peak (200) into two tetragonal ordered $L1_0$ phase peaks – (200) and (002). Based on the resistometry and X-ray diffraction analysis data, the authors carried out a quantitative assessment of the rate of the disorder→order phase transformation in the alloy under the study. It is established that the values of the transformed volume fraction (resistometry) and the long-range order degree (X-ray diffraction analysis) are close. The study shows that in the temperature range of 200–250 °C, the rate of atomic ordering according to the $L1_0$ type in the nonstoichiometric alloy Cu–56 at. % Au is maximum at 250 °C. It is identified that the disorder→order transformation in the initially quenched specimens of the investigated alloy proceeds approximately an order of magnitude faster than in preliminarily deformed specimens.

Keywords: Cu–56 at. % Au; Cu-Au alloys; atomic ordering; resistometry; superstructural X-ray reflections; order degree evaluation.

For citation: Podgorbunskaya P.O., Zgibnev D.A., Gavrilova A.A., Novikova O.S., Volkov A.Yu. The kinetics of L_10 superstructure formation in the Cu–56Au alloy (at. %): resistometric study. *Frontier Materials & Technologies*, 2023, no. 3, pp. 83–94. DOI: 10.18323/2782-4039-2023-3-65-8.

INTRODUCTION

The formation of an atomically ordered crystal lattice was discovered by Russian scientists more than 100 years ago, when studying the structure formed in a gold-copper alloy as a result of slow cooling from high temperature [1]. Since then, the formation of the structure and properties in the system of gold – copper alloys has been repeatedly studied in detail using various research techniques [2–4]. In the work [2], the authors studied the diffraction patterns, and obtained the concentration dependence of the specific electrical resistivity of the equiatomic CuAu alloy in various structural states. The formation of a lamellar structure in the CuAuI alloy in the temperature range of 270–370 °C

was recorded in [3]. The lamellar structure consists of colonies of lamellar *c*-domains, where within one colony, the domains are in a twin orientation relative to the plane of their boundary {110}. As [5] shows, planes of this particular type are the planes of optimal conjugation in the fcc→fct transition. In [6], using the molecular dynamics method, computer experiments were carried out for the estimated block of an ordered CuAuI alloy with the $L1_0$ superstructure. It was shown that during thermal activation, if there are single vacancies in the alloy, they will tend to form vacancy complexes, for example, divacancies. The EBSD analysis of the CuAu alloy microstructure, was successfully used, to study the $L1_0$ phase orientations in the $A1$ matrix and showed the following orientation relationships:

(101)$L1_0$//{110}$A1$ and [010]$L1_0$//[010]$A1$ [7]. The lamellar structure is also observed during the formation of a long-period ordered phase of the CuAuII type [4]. A rather detailed analysis of the features of atomic ordering in the system of Cu–Au alloys is given in [8], which also presents an improved phase diagram and gives a crystallographic description of the formed ordered structures. The increased interest in these alloys is caused not only by the need to clarify the crystallography of the transformation of a disordered crystal lattice into an atomically ordered one. The fact is that gold-copper alloys are the basis of materials for various practical applications: this is both jewellery or dentistry and corrosion-resistant alloys for tool engineering [5; 9]. A detailed description of all areas of application of gold–copper alloys with references to relevant sources is given in [10].

According to the phase diagram of the Cu–Au system, upon cooling from high temperatures, several structural-phase transformations occur in alloys close to the equiatomic composition. First, near 400 °C, in the disordered fcc structure ($A1$-phase), an orthorhombic ordered CuAuII phase is formed, which, upon further cooling, rearranges into the ordered CuAuI phase. There are coexistence regions between these phases: ($A1$+CuAuII) and (CuAuI+CuAuII) [8]. A schematic view of the crystal lattice ordered according to the CuAuI-phase type is shown in Fig. 1. The orthorhombic CuAuII phase crystal lattice can be represented as 10 CuAuI phase crystal lattices, arranged together along the *a*-axis with an antiphase shear-type boundary in the middle.

The (100) type planes of the CuAuI phase crystal lattice are periodically filled with either gold or copper atoms (Fig. 1). Therefore, the initial fcc lattice becomes tetragonal as a result of atomic ordering, and the tetragonal *c*-axis is perpendicular to the lamination direction. At the same time, the lattice parameter slightly increases along the *a* and *b* axes, and decreases along the *c* axis. Such a rearrangement leads to the fact that the disorder→order phase transition in gold-copper alloys is accompanied by a decrease in the crystal lattice volume by approximately 1 % causing strong internal stresses. Shape distortion or even spontaneous destruction of jewellery due to atomic ordering, has been described in the literature [9; 11] many times. The scientific basis for solving problems with distortion or

cracking of gold products, is given in [5] using the example of a detailed study of the structure and properties of the equiatomic Cu–50Au alloy in various structural states.

Previously, the equiatomic Cu–50Au (at. %) alloy was studied in most detail. Fewer works study alloys with a small deviation from stoichiometry. In the work [12], high-temperature *in situ* X-ray diffraction and mechanical spectroscopy, were applied to study phase transitions in the Au–25 wt. % Cu alloy when heating and cooling at a rate of 1 K/min (note that this composition corresponds with high accuracy to the equiatomic Cu–50Au alloy). Upon continuous heating, the following sequence of phase transitions was recorded: $A1$→AuCuI→AuCuII→$A1$, and upon subsequent cooling: $A1$→$A1$+AuCuI+AuCuII→AuCuI+AuCuII→AuCuI. In [13], the influence of plastic deformation on the ordered and disordered jewellery "red gold" alloy of the Cu–Au–Ag composition is described. It was identified that preliminary deformation reduces the temperature of the ordering process onset. However, this result can be explained by the influence of silver precipitation on the transformation acceleration [14]. In the work [15], the authors studied a method for determining the phase composition on the Cu (9.38%)–Au (90.62%) and Au (74.11%)–Cu (25.89%) alloys using laser-induced breakdown spectroscopy. Using the molecular dynamics method, the work [16] presents the results of computer simulation of the synthesis of binary Cu–Au nanoclusters, upon condensation from a high-temperature gaseous medium of Cu_3Au, CuAu, Cu90Au10, and Cu60Au40 chemical compositions. The theoretical possibility of the formation of binary Cu–Au clusters of a certain size with a certain predetermined chemical composition from the gas phase was established.

There are practically no publications dealing with the study of the structure and properties of gold-copper alloys with a deviation from stoichiometry of more than 5 %. Meanwhile, such alloys are of interest for various technical applications, for example, for the production of conductors of weak electrical signals operating in highly corrosive media. For example, the Cu–56Au alloy (at. %) is mass-produced under the ZlM-80 brand. However, the kinetics of the disorder→order transition in this alloy has been barely studied. It was found in [17] that the maximum rate of atomic ordering in the Cu–56Au (at. %) alloy falls within the temperature range of 300–350 °C,
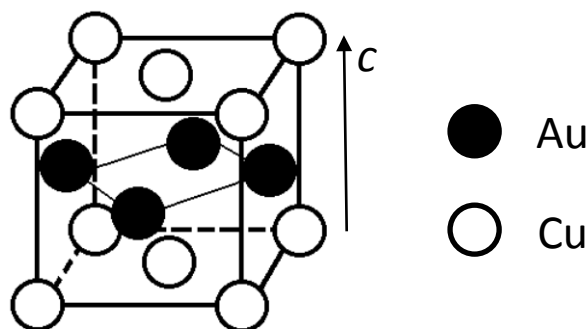

Fig. 1. *Schematic view of the crystal lattice of the ordered CuAuI phase*
Рис. 1. *Схематическое изображение кристаллической решетки атомно-упорядоченной фазы СиAuI*

and the orthorhombic ordered CuAuII phase is formed in this case. The work [14] shows that the rate of the Cu–56Au alloy ordering is much lower than that of the equiatomic CuAu alloy. It was established that slow (at a rate of 12 deg/h) cooling from 600 °C to room temperature is the fastest way to form an ordered state in the Cu–56Au alloy. However, as a result of such treatment, the high-temperature CuAuII phase appears in the alloy and not the equilibrium CuAuI phase, which is expected on the basis of the phase diagram. It is shown that the orthorhombic ordered CuAuII phase formed in the alloy has a high thermal stability, and is retained even after long-term low-temperature annealing. Thus, the kinetics of the formation of the low-temperature ordered CuAuI phase in the Cu–56Au alloy has not yet been studied in detail.

The purpose of this work is to find out the rate of atomic ordering of the $L1_0$ type in the Cu–56Au alloy in the temperature range of 200–250 °C.

METHODS

For the study, an alloy was taken, which contains 56 at. % of gold and 44 at. % of copper (or 80 wt. % Au and 20 wt. % Cu). According to the Cu–Au system phase diagram [8], the disorder→order phase transition in the alloy under study occurs at temperatures below 375 °C. Therefore, the initial, disordered state in the alloy samples was formed by quenching from a temperature of 600 °C after annealing for 1 h. Moreover, the authors studied the influence of preliminary plastic deformation on the kinetics of atomic ordering. In this case, the initial disordered state was formed by the deformation of the samples by 90 %.

The study of the transformation kinetics in this work was carried out in the temperature range of 200–250 °C. The duration of heat treatments during the study ranged from 1 h to 2 months. All heat treatments were carried out in evacuated glass or quartz ampoules.

As the main research technique in our work, resistometry was chosen. Electrical resistivity at room temperature was measured, using the standard four-probe method on long wire samples with a diameter of 0.25 mm at a constant current I=20 mA. The measurement accuracy was ±0.04·10⁻⁸ Ohm·m. Moreover, the temperature dependences of the electrical resistivity during heating and cooling of the samples at a constant rate of 120 deg/h were constructed.

Based on the resistometry data, the authors estimated the relative volume of the new phase using the formula

$$\eta = \frac{\rho_{dis} - \rho_t}{\rho_{dis} - \rho_{LRO}},$$

where η is the transformed volume fraction;
ρ_{dis} and ρ_{LRO} are the specific electrical resistivity values of samples in the state of disorder and long-range order (LRO), respectively;
ρ_t is the specific electrical resistivity of the sample at a certain stage of heat treatment.

X-ray diffraction analysis (hereinafter referred to as XRD) was carried out on the alloy plates 0.3 mm thick using a PANalytical Empyrean Series 2 diffractometer in Cu-Kα radiation. To determine the LRO degree, the ratio of the integral intensities of the superstructural and fundamental peaks was calculated using known formulas [18; 19]. Calculations were carried out for several pairs of reflections, after which the average value was determined. Such an approach is necessary to minimise the influence of texture effects on the result. X-ray diffraction calculations were carried out only after annealings of maximum duration.

RESULTS

Fig. 2 shows the Temperature dependences of electrical resistivity obtained during heating of initially deformed (Fig. 2 a) or quenched (Fig. 2 b) samples of the Cu–56Au alloy after annealings of various durations (from 1 h to 2 months) at a temperature of 250 °C. Note that some of the temperature dependences we obtained are not shown in Fig. 2: at long exposure times, the electrical resistivity of the samples changes insignificantly, so the curves begin to overlap each other.

The electrical resistivity of the Cu–56Au alloy disordered by quenching is ρ=14.29·10⁻⁸ Ohm·m. An alloy disordered by severe plastic deformation (90 %) has a lower electrical resistivity – ρ=14.06·10⁻⁸ Ohm·m.

Comparison of temperature dependences given in Fig. 2 shows that the decrease in electrical resistivity caused by atomic ordering occurs somewhat faster, in the quenched sample. For example, when an initially deformed sample is heated, the dependence remains almost linear up to 200 °C. In turn, in the quenched sample, a slight drop in electrical resistivity begins at about 150 °C. Continued heating leads to a gradual decrease in electrical resistivity. The electrical resistivity minimum values are achieved at a temperature of ~320 °C regardless of the initial state of the samples. Further heating causes a rather sharp increase in electrical resistivity, which is caused by a change in the alloy phase composition: CuAuI→CuAuII→$A1$. At temperatures above 380 °C, the alloy becomes single-phase and disordered, which results in a linear dependence of the electrical resistivity.

All the transformations described above are quite clearly identified on the graphs of the temperature derivatives of the corresponding electrical resistivity dependences (Fig. 3). In Fig. 3 a, two peaks are revealed in the temperature range of 300–400 °C. The first of them, with a maximum at about 350 °C, corresponds to the CuAuI→CuAuII transformation. The second peak, whose maximum falls at ~380 °C, corresponds to the CuAuII→$A1$ transformation. When comparing the dependencies in Fig. 3 a, it is well seen that in the pre-quenched sample, these peaks are clearly separated and have a higher intensity.

Fig. 2 clearly shows that after annealings of the same duration, the specific electrical resistivity of pre-quenched samples is always lower. After annealing of the quenched alloy for 2 months at a temperature of 250 °C, its specific electrical resistivity decreases to ρ=7.04·10⁻⁸ Ohm·m. As follows from Fig. 2, after annealing of the same duration, the initially deformed sample has a significantly higher value of electrical resistivity. Consequently, a LRO state has not yet formed in this sample. What calls attention is the fact that after annealings of the maximum duration, clearly pronounced steps are observed in the temperature dependences of the electrical resistivity (shown in the insets in Fig. 2 a and 2 b). They are especially visible after annealing of pre-quenched samples. The difference, in reaction rates at different temperatures, is clearly seen in the graphs of
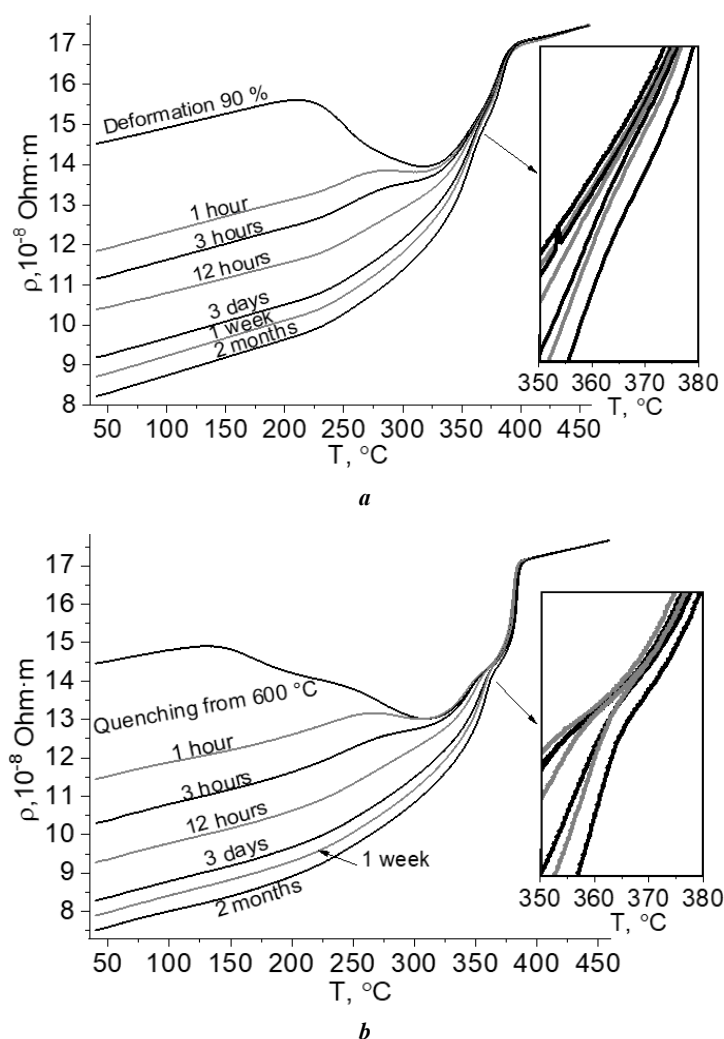
Fig. 2. *Temperature dependences of electrical resistivity obtained when heating the deformed (**a**)*
*and quenched (**b**) specimens of the Cu–56Au alloy, which were annealed at a temperature of 250 °C from 1 h to 2 months.*
The insets show the regions where the step change in the electrical resistance is observed
Рис. 2. *Температурные зависимости электросопротивления, полученные при нагреве деформированных (**a**)*
*и закаленных (**b**) образцов сплава Cu–56Au, которые отжигались при температуре 250 °C от 1 ч до 2 мес.*
На вставках показаны участки, на которых наблюдается ступенчатое изменение электросопротивления

temperature derivatives (Fig. 3 b). The narrow and intense peaks in the graphs of the temperature derivatives of the electrical resistivity, once again confirm the higher degree of atomic order achieved as a result of annealing of the pre-quenched alloy.

Fig. 4 shows XRD patterns of samples in two initial states, as well as after their annealing for 1 h and 2 months at 250 °C.

According to the data obtained, the lattice parameter of the 90 % deformed Cu–56Au alloy is a=0.3912 nm. The X-ray peaks of the deformed alloy are quite wide, which is caused by elastic stresses and a large number of nonequilibrium boundaries [20]. Annealing at a high temperature relieves stress, and reduces the structure defect, as a result of which the crystal lattice parameter of the quenched alloy decreases to a=0.3901 nm. Compared to the deformed state, the X-ray peaks of the quenched alloy are very narrow and have a high intensity (one can compare XRD patterns 1 in Fig. 4 a and 4 b).

The ordered arrangement of atoms in the crystal lattice changes the conditions for X-ray reflection, as a result of which the number of peaks in the diffraction patterns of annealed samples increases significantly. Peaks (001), (011), etc. appear, which are forbidden for the fcc structure. Such additional peaks are called superstructural, and the ordered lattice itself is called a superstructure. Moreover, additional fundamental peaks appear in the XRD patterns of the $L1_0$ superstructure. For example, the original fundamental peak (200) is split into two peaks – (200) and (002). This is caused by the rearrangement of the initial disordered fcc lattice into an ordered tetragonal structure (Fig. 1). According to the obtained XRD data, annealing of the quenched alloy for 2 months at a temperature of 250 °C leads to the formation of an $L1_0$ superstructure, the crystal lattice of which has the following parameters: a=0.3963 nm and c=0.3671 nm.

Since the crystal lattice parameter along the a and b axes slightly increases during atomic ordering, the reflections
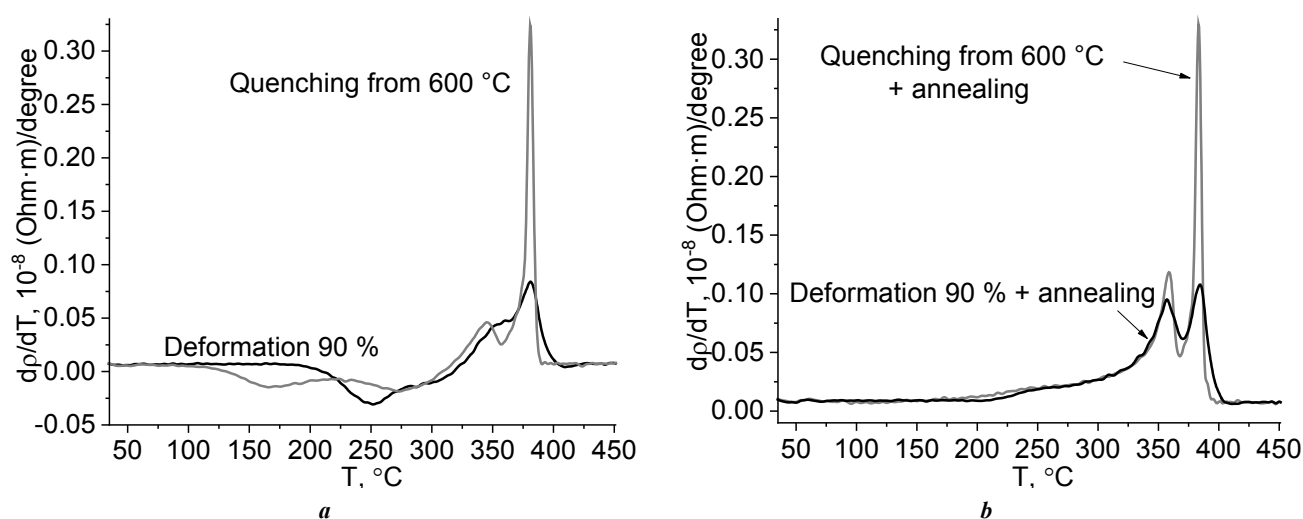
Fig. 3. *Temperature derivatives of the electrical resistivity dependences (Fig. 2)*
*obtained when heating specimens of the Cu–56Au alloy in two initial states (**a**)*
*and after annealing of these specimens at a temperature of 250 °C during 2 months (**b**)*
Рис. 3. *Температурные производные зависимостей электросопротивления (рис. 2),*
*полученные при нагреве образцов сплава Си–56Аи в двух исходных состояниях (**a**)*
*и после отжигов этих образцов при температуре 250 °С в течение 2 мес. (**b**)*

from these planes shift to the left of the original peak. In turn, the new peak (002) is a reflection from the planes, the interplane distance between which (along the *c*-axis) is less than the original one, in consequence of which this peak is formed to the right of the original one. Obviously, in the equilibrium state, the intensity of the $(200)L1_0$ peak should be two times higher than that of the $(002)L1_0$ peak. In Fig. 4, this condition is practically met only for the sample that was annealed after preliminary quenching. In full accordance with the resistometric data, annealing of the sample, initially deformed for 2 months at 250 °C does not lead to a diffraction pattern corresponding to a well-ordered state.

The curves in Fig. 5 show the change in the electrical resistivity of the alloy under study during long-term heat treatments in the selected temperature range. Due to differences in the mechanisms of formation of an ordered structure, these dependences are plotted separately for the initially deformed and pre-quenched states of the alloy. At the annealing temperature of 250 °C, the left points (i.e., at room temperature) on the corresponding temperature dependences of the electrical resistivity were taken to construct these graphs (Fig. 2).

As follows from the graphs in Fig. 5, regardless of the initial state, the rate of decrease in electrical resistivity during annealing is maximum at a temperature of 250 °C. Based on this, one can make an unambiguous conclusion that the rate of the disorder→order phase transition at this temperature is maximal as well. In turn, the rate of decrease in electrical resistivity at a temperature of 200 °C is minimal.

Fig. 6 shows XRD patterns obtained from samples that were held for 2 months at temperatures of 200, 225, and 250 °C. Note that, regardless of the annealing temperature, diffraction patterns with more intense peaks correspond to pre-quenched samples. A quenched sample annealed at a temperature of 250 °C has the clearest pattern of X-ray

reflections, fully corresponding to a LRO structure with the $L1_0$ type. Thus, the conclusions made based on the resistometry data are again well confirmed by the X-ray diffraction data.

Fig. 6 clearly shows that the XRD patterns from the samples annealed at 200 °C, do not have some peaks typical of the ordered state (for example, (002)). This means that the phase transition at this temperature is still far from completion. Such a slow phase transition rate allows tracing the initial stages of the rearrangement of the disordered fcc structure into the $L1_0$ ordered one. Fig. 7 shows the initial $(200)A1$ peak splitting into two peaks – $(200)L1_0$ and $(002)L1_0$ (in the range of 2θ angles from 44 to 50°), which gives the clearest picture of the ordered structure formation. Previously, similar experiments were carried out on the equiatomic CuAu alloy [21]. However, the high transition rate did not allow observing all the structural rearrangement stages.

As follows from the data shown in Fig. 7, a shoulder appears on the left side of the initial peak (200) at the first stage of ordering. Therefore, *a* and *b* planes of the ordered phase, which have a larger interplanar spacing compared to the disordered matrix, are first formed. The $(002)L1_0$ peak, which is formed from tetragonal *c*-planes with a smaller parameter, becomes clearly visible only after 1 month of annealing at a temperature of 200 °C. In Fig. 7, the different rates of the ordered structure formation in the deformed and quenched samples again are clearly revealed. Here, one can also compare the different widths of X-ray reflections from heavily deformed or quenched samples.

The set of results obtained in this work allows quantifying the rate of the disorder→order phase transition in the alloy under study in the temperature range of 200–250 °C (Fig. 8).

Moreover, the LRO degree *(S)*, averaged over the sample, can be estimated based on the XRD-data in Fig. 6. Note that both considered parameters (η and *S*) have the same physical
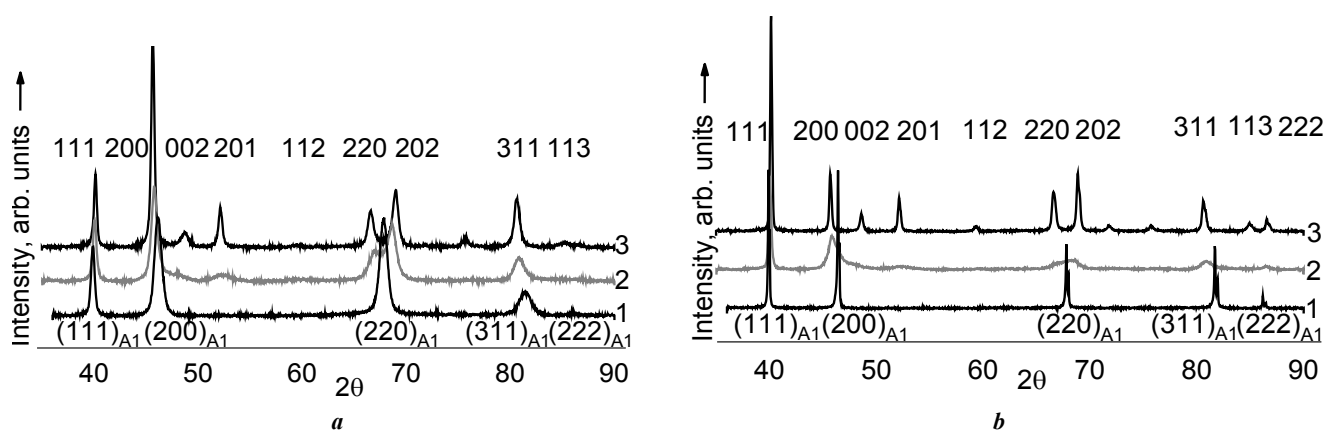
Fig. 4. *The results of XRD analysis of specimens of the deformed (**a**) and quenched (**b**) alloy in the initial states (1),*
after annealing during 1 h (2) and 2 months (3) at 250 °C
Рис. 4. *Результаты РСА-исследования образцов деформированного (**a**) и закаленного (**b**) сплава в исходных состояниях (1),*
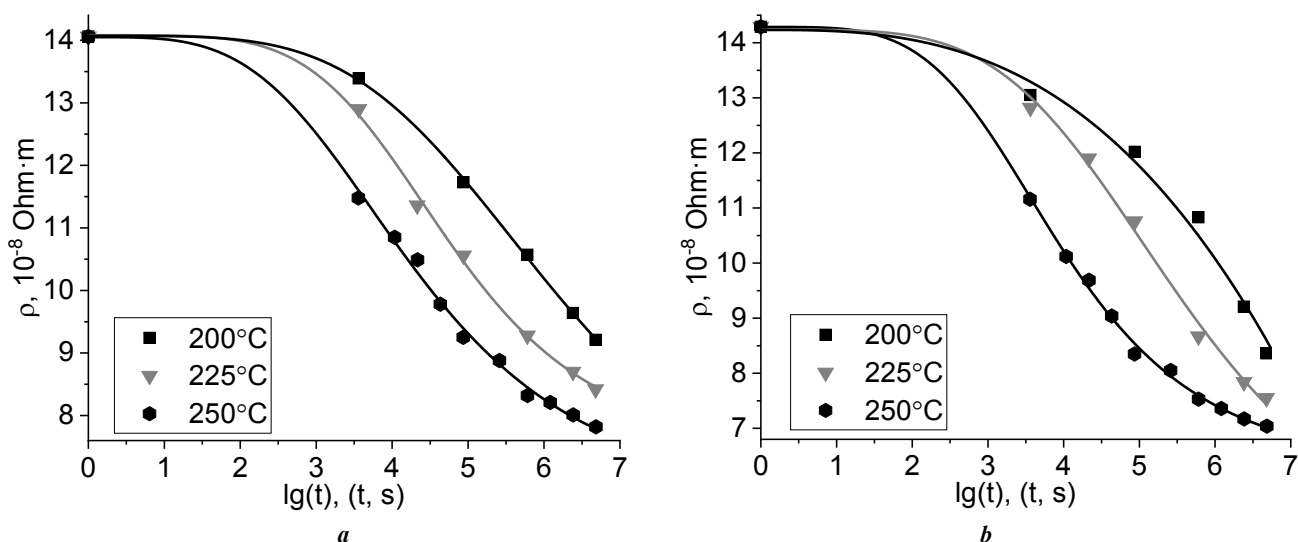*после отжига в течение 1 ч (2) и 2 мес. (3) при 250 °C*

Fig. 5. *Change in the specific electrical resistance of the initially deformed (**a**) and quenched (**b**) specimens of the alloy*
under study in the process of annealing at temperatures of 200, 225, and 250 °C
Рис. 5. *Изменение удельного электросопротивления исходно деформированных (**a**) и закаленных (**b**) образцов*
исследуемого сплава в процессе отжигов при температурах 200, 225 и 250 °C

significance, and differ only in the method on the basis of which they were obtained. The values of the LRO degree determined, based on the XRD-data, are shown by points in Fig. 8. Moreover, due to the insufficient number of super-structural peaks, we failed to estimate the fraction of the transformed volume after annealing of the deformed sample at temperatures of 200 and 225 °C.

DISCUSSION

Previously, we assumed [14] that annealing at 250 °C is optimal for the $L1_0$ superstructure formation in the Cu–56Au alloy. It was found as well that holding at this temperature for 1 week is far from sufficient for the formation of a well-ordered state in this alloy. The study completely confirmed the previously obtained conclusions, and showed that to complete the disorder→order phase transition, it is

necessary to anneal the nonstoichiometric Cu–56Au alloy for at least 2 months at 250 °C. Lowering the processing temperature significantly, slows down the transition rate. In addition, it was reliably identified that the atomic ordering rate depends heavily on how the initial, disordered state was formed in the alloy: by quenching from high temperature or by plastic deformation.

All the obtained results indicate that the rate of ordering of pre-quenched samples is higher in the studied temperature range. This seems unusual, since plastic deformation significantly increases the rate of diffusion reactions [22]. For example, the rate of ordering of preliminarily deformed alloys is higher, as a rule [18; 23]. Thus, the phenomenon of a decrease in the ordering rate after preliminary deformation observed in the Cu–56Au alloy requires an explanation.

As was shown in [24], by high-resolution electron microscopy, clusters 2–3 nm in size with a high LRO degree,
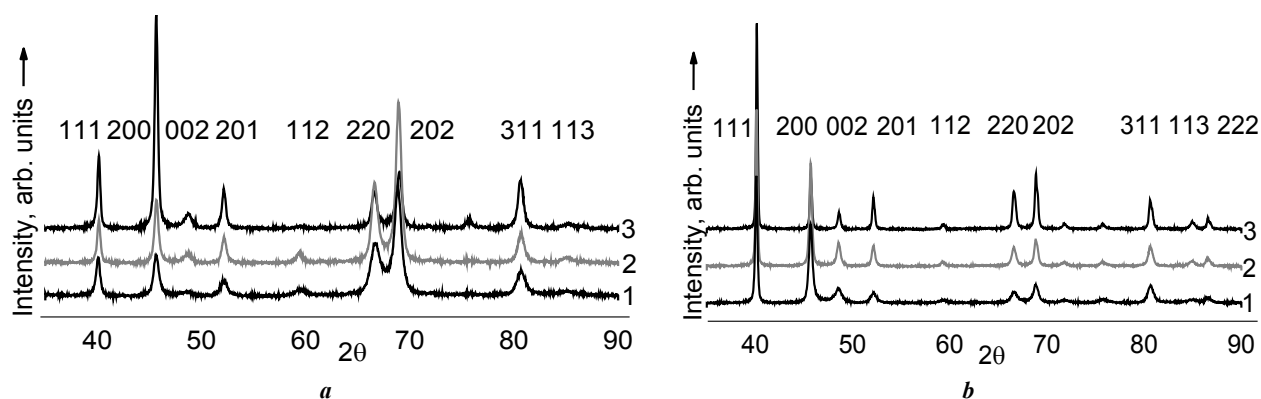
Fig. 6. *X-ray diffraction patterns obtained from the initially deformed (**a**) and quenched (**b**) specimens*
annealed during 2 months at temperatures of 200 (1), 225 (2), and 250 °C (3)
Рис. 6. *Рентгеновские дифрактограммы, полученные с исходно деформированных (**a**) и закаленных (**b**) образцов,*
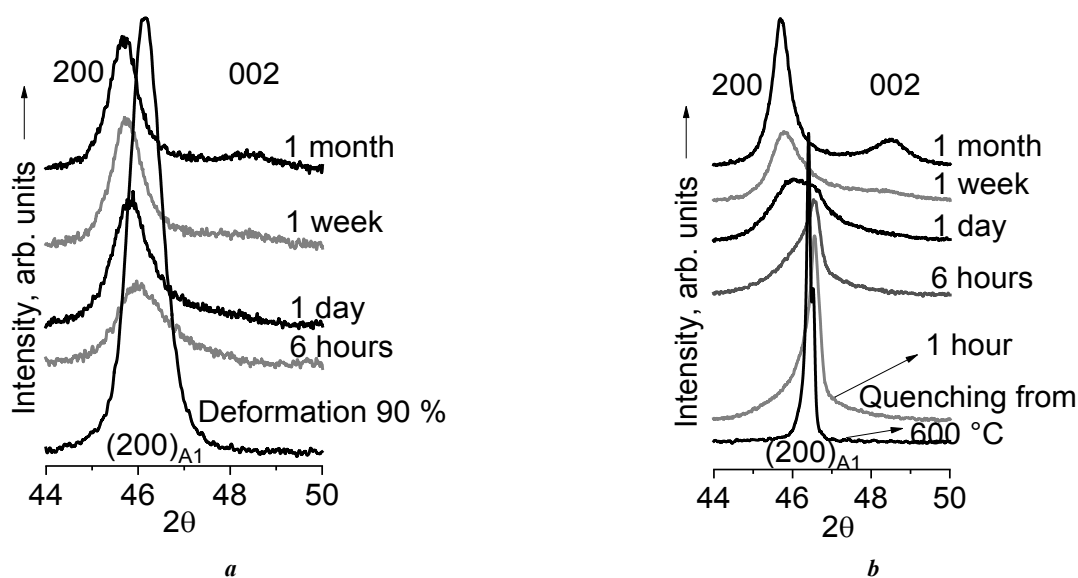*отожженных в течение 2 мес. при температурах 200 (1), 225 (2) и 250 °C (3)*

Fig. 7. *X-ray reflection (200) evolution during atomic ordering at a temperature of 200 °C*
*of the initially deformed (**a**) and quenched (**b**) specimens*
Рис. 7. *Эволюция рентгеновского отражения (200) в ходе атомного упорядочения при температуре 200 °C*
*исходно деформированных (**a**) и закаленных (**b**) образцов*

are formed in gold-copper alloys even during quenching. The number of these clusters is determined by the temperature and quenching rate. Cases when quenching of gold-copper alloys led to the formation of a strong short-range order in them have been described in the literature many times. In this case, in addition to strong reflections from the disordered fcc phase, the XRD patterns show the extended maxima at the positions of superstructural reflections (as an example, see Fig. 1 a in [12]). The formation of ordered nanoclusters in the alloy, during quenching, also leads to a significant increase in electrical resistivity (initial points in Fig. 2 a and 2 b). Plastic deformation destroys these clusters, as a result of which the alloy electrical resistivity decreases [23; 25].

In turn, in a strongly deformed alloy, a combined reaction occurs: the atomic ordering process is accompanied by recrystallisation. The paper [26] describes the possible options:

either ordering and recrystallisation are implemented jointly, or one of these solid-state reactions overtakes the other. Most often, the boundary of a growing recrystallised grain is simultaneously an interphase boundary [27]. The progress of recrystallisation can be judged from the decrease in the width of X-ray peaks during annealing of the deformed alloy. Indeed, it is clearly seen in Fig. 7 a that when increasing the duration of heat treatment of the initially deformed alloy, the broad peak (200) gradually becomes narrower.

Thus, the difference in the rates of disorder→order transition is caused by the difference in the mechanisms of the ordered state formation in quenched or deformed samples of the same alloy. Even a slight heating of a quenched sample leads to the fact that the ordered clusters in it become the nuclei of a new phase. In turn, to initiate the phase transition in a deformed alloy, it must be heated to the recrystallisation temperature.
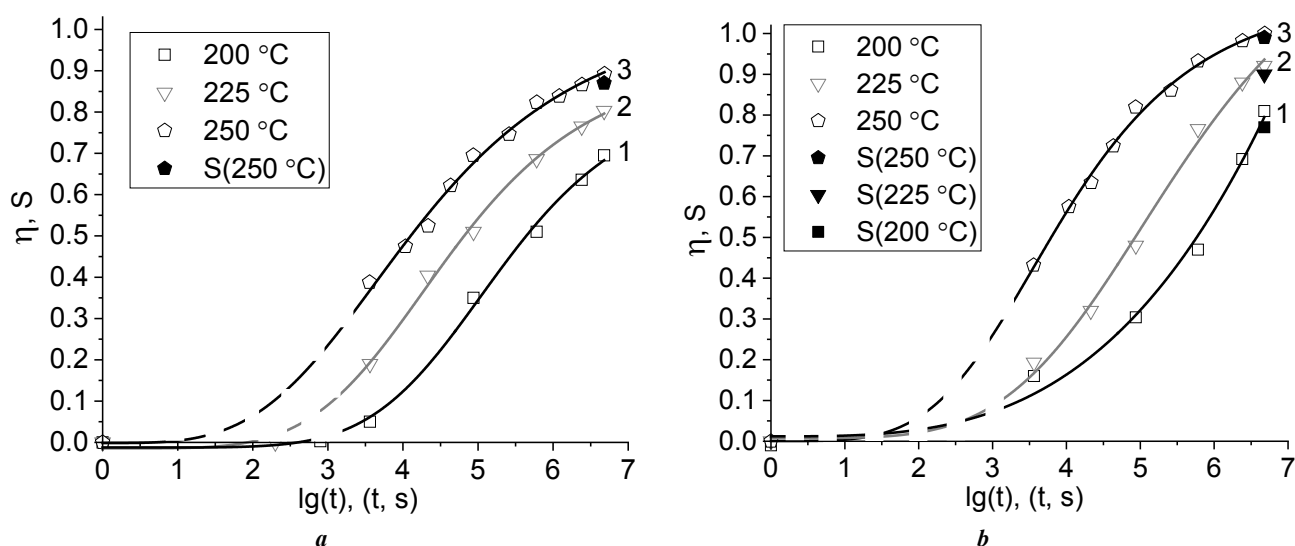
Fig. 8. *The transformed fraction as a function of the annealing time of the deformed (**a**)*
*and quenched (**b**) specimens of the Cu–56Au alloy at temperatures of:*
200 (1), 225 (2), and 250 °C (3) built according to the resistometry data.
Evaluation based on the XRD-results was carried out after maximum duration annealing and is shown by points
Рис. 8. *Изменение доли превращенного объема от продолжительности отжига деформированных (**a**)*
*и закаленных (**b**) образцов сплава Cu–56Au при температурах:*
200 (1), 225 (2) и 250 °C (3), построенные по данным резистометрии.
Оценки на основе РСА-результатов проводились после отжигов максимальной продолжительности и показаны точками

Of course, the results obtained during resistometry of the alloy samples after maximum duration annealings are of special interest. As mentioned above, the minimum electrical resistivity of the Cu–56Au alloy achieved in this work is $\rho=7.04 \cdot 10^{-8}$ Ohm·m. It was obtained by annealing of a quenched alloy for 2 months at a temperature of 250 °C. To verify the result obtained, an additional annealing of this sample was carried out for another 2 months. This processing slightly influenced the value of electrical resistivity, which amounted to $\rho=6.98 \cdot 10^{-8}$ Ohm·m. This allows concluding that to complete the disorder→order phase transition in the Cu–56Au alloy at a temperature of 250 °C, annealing for 2 months is required. Note that the electrical resistivity values obtained during the study are quite lower than the known literature data. Previously, we have already concluded that the generally accepted concentration dependence of the electrical resistivity of the Cu–Au system alloys (see Fig. 46 in [9]) needs to be refined [28].

The results of the XRD study of the nonstoichiometric Cu–56Au alloy obtained in our work can be compared with the literature data [29] given for the stoichiometric Cu–50Au alloy. For example, the crystal lattice parameters of an equiatomic alloy ordered after the $L1_0$ type (a=0.3958 nm, c=0.3666 nm) are somewhat smaller than those under study. However, the tetragonality degrees of the ordered lattices of both alloys are equal and amount to c/a=0.926. This is a rather interesting result that will allow reasoning about the structure of a nonstoichiometric alloy at the atomic level. Indeed, when deviating from stoichiometry, the question always arises: how the excess number of atoms (in this case, gold) is redistributed during the superlattice formation. If we assume that some of the gold atoms are embedded in the copper sublattice, this should lead to a difference in the tetragonality degrees of the crystal lattices of

the alloys. Most likely, in the process of atomic ordering, an excess amount of gold atoms is displaced onto defects and boundaries of various nature (for example, *c*-domain boundaries, thermal antiphase domain boundaries (APBs), shear-type APBs, grain boundaries, etc.). This is indirectly confirmed by the higher strength (by ~15 %) of the ordered nonstoichiometric alloy compared to the equiatomic one. This hypothesis was put forward for the first time and requires verification using structural research methods (for example, high-resolution electron microscopy).

The study showed that the results of a quantitative assessment of the phase transition rate ($A1{\rightarrow}L1_0$) based on the resistometry and XRD data are close (Fig. 8). This makes it possible, using two methods, to compare the rate of atomic ordering of nonstoichiometric alloy samples in different initial states. For example, the fraction of the transformed volume after the deformed alloy annealing at a temperature of 250 °C for 2 months is η=0.89 (according to resistometric data) or S=0.87 (according to X-ray diffraction data). In the initially quenched alloy, similar values of the transformed volume fraction are achieved after annealing for ~4 days (i.e., an order of magnitude faster).

CONCLUSIONS

1. It was established that the formation of the $L1_0$ superstructure in the initially quenched nonstoichiometric Cu–56Au alloy, occurs approximately an order of magnitude faster than in the pre-deformed alloy.

2. It was identified that in the temperature range of 200–250 °C the maximum rate of ordering of the nonstoichiometric Cu–56Au alloy is observed at 250 °C; however, even in this case 2 months' exposure is necessary to form a LRO state with $L1_0$ superstructure.

3. It was suggested that during the disorder→order phase transition, excess (compared to stoichiometry) gold atoms are not built into the copper sublattice, but are displaced onto domain walls and other defects.

4. Based on the obtained data, for the first time for the Cu–56Au alloy, kinetic C-curves can be plotted and the thermodynamic n and k constants calculated in the temperature range of 200–250 °C for the disorder→order transition ($A1→L1_0$).

REFERENCES

1. Kurnakov N., Zemczuzny S., Zasedatelev M. Transformations in Alloys of Gold with Copper. *Journal of the Institute of Metals*, 1916, vol. 15, pp. 305–331.

2. Jogansson C.H., Linde J.O. Röntgenographische und elektrische Untersuchungen der CuAu-Systems. *Annalen der Physik*, 1936, vol. 417, no. 1, pp. 1–48. DOI: 10.1002/andp.19364170102.

3. Hirabayashi M. Stress-Ordering Effect on Thermal Expansion of CuAu Single Crystals. *Journal of the Physical Society of Japan*, 1959, vol. 14, pp. 149–152. DOI: 10.1143/JPSJ.14.149.

4. Van Tendeloo G., Amelinckx S., Jeng S.J., Wayman C.M. The initial stages of ordering in CuAuI and CuAuII. *Journal of Materials Science*, 1986, vol. 21, pp. 4395–4402. DOI: 10.1007/BF01106562.

5. Getov L.A., ed. *Khudozhestvennoe litye iz dragotsennykh metallov* [Artistic casting from precious metals]. Leningrad, Mashinostroenie Publ., 223 p.

6. Popova L.A. Structural and energy properties of bivacansions in CuAu alloy. *Yugra state university bulletin*, 2022, vol. 66, no. 3, pp. 145–151. DOI: 10.18822/byusu202203145-151.

7. Larcher M., Cayron C., Blatter A., Soulignac R., Logé R.E. Electron backscatter diffraction study of variant selection during ordering phase transformation in L1₀-type red gold alloy. *Journal of Applied Crystallography*, 2019, vol. 52, pp. 1202–1213. DOI: 10.1107/S1600576719011890.

8. Fedorov P.P., Volkov S.N. Au-Cu phase diagram. *Russian journal of inorganic chemistry*, 2016, vol. 61, no. 6, pp. 809–812. DOI: 10.7868/S0044457X16060061.

9. Malyshev V.M., Rumyantsev D.V. *Zoloto* [Gold]. Moscow, Metallurgiya Publ., 1979. 288 p.

10. Trong D.N., Long V.C., Saraç U., Quoc V.D., Ţălu Ş. First-Principles Calculations of Crystallographic and Electronic Structural Properties of Au-Cu Alloys. *Journal of Composites Science*, 2022, vol. 6, no. 12, pp. 383. DOI: https://doi.org/10.3390/jcs6120383.

11. Volkov A.Y., Kazantsev V.A. Impact of the initial state on the structure and properties of the ordered CuAu alloy. *The physics of metals and metallography*, 2012, vol. 113, no. 1, pp. 66–76. DOI: 10.1134/S0031918X12010127.

12. Lamiri I., Martinez-Blanco D., Abdelbaky M.S.M., Mari D., Hamana D., García-Granda S. Investigation of the order-disorder phase transition series in AuCu by in-situ temperature XRD and mechanical spectroscopy. *Journal of Alloys and Compounds*, 2019, vol. 770, pp. 748–754. DOI: 10.1016/j.jallcom.2018.08.094.

13. Garcia-Gonzalez M., Van Petegem S., Baluc N., Hocine S., Dupraz M., Lalire F., Van Swygenhoven H. Enhanced precipitate growth at reduced temperatures during chemical ordering in deformed red gold alloys. *Scripta Materialia*, 2019, vol. 170, pp. 129–133. DOI: 10.1016/j.scriptamat.2019.05.038.

14. Volkov A.Yu., Antonova O.V., Glukhov A.V., Komkova D.A., Antonov B.D., Kostina A.E., Livinets A.A., Generalova K.N. Features of the disorder-order phase transition in non-stoichoimetric Cu-56at%Au alloy. *Journal of Alloys and Compounds*, 2022, vol. 891, p. 161938. DOI: 10.1016/j.jallcom.2021.161938.

15. Farooq Z., Ali R., Ahmed N., Fahad M., Ahmad A., Yaseen M., Mahmood M.H.R., Hussain S., Rehan I., Zubair Khan M., Jan T., Qayyum M.A., Afzal M., Mahr M.S., Shafique M. Determination of the Gold Alloys Composition by Laser-Induced Plasma Spectroscopy Using an Algorithm for Matching Experimental and Calculated Values of Electron Number Density. *Journal of Applied Spectroscopy*, 2023, vol. 90, pp. 126–136. DOI: 10.1007/s10812-023-01513-x.

16. Gafner Y.Y., Gafner S.L., Golovenko Z.V. Analysis of the size distribution of binary Cu-Au nanoparticles during synthesis from a gaseous medium. *Letters on Materials*, 2020, vol. 10, no. 1, pp. 33–37. DOI: 10.22226/2410-3535-2020-1-33-37.

17. Generalova K.N., Glukhov A.V., Volkov A.Y. Kinetics of atomic ordering by L1₀-type in non-stoichiometric copper-gold alloy: X-ray analysis. *Bulletin of Perm national research polytechnic university. Mechanical engineering, materials science*, 2018, vol. 20, no. 2, pp. 75–85. DOI: 10.15593/2224-9877/2018.2.09.

18. Volkov A.Yu., Novikova O.S., Antonov B.D. The kinetics of ordering in an equiatomic CuPd alloy: A resistometric study. *Journal of Alloys and Compounds*, 2013, vol. 581, pp. 625–631. DOI: 10.1016/j.jallcom.2013.07.132.

19. Glezer A.M., Timshin I.A., Shchetinin I.V., Gorshenkov M.V., Sundeev R.V., Ezhova A.G. Unusual behavior of long-range ordered parameter in Fe₃Al superstructure under severe plastic deformation in Bridgman anvils. *Journal of Alloys and Compounds*, 2018, vol. 744, pp. 791–796. DOI: 10.1016/j.jallcom.2018.02.124.

20. Valiev R.Z., Aleksandrov I.V. *Nanostrukturnye materialy, poluchennye intensivnoy plasticheskoy deformatsiey* [Nanostructured materials obtained by severe plastic deformation]. Moscow, Logos Publ., 2000. 271 p.

21. Malis O., Ludwig K.F. Kinetics of phase transitions in equiatomic CuAu. *Physical Review B*, 1999, vol. 60, no. 21, pp. 14675–14682. DOI: 10.1103/PhysRevB.60.14675.

22. Christian J.W. *Teoriya prevrashcheniy v metallakh i splavakh* [The theory of transformation in metals and alloys]. Vol. 1. Moscow, Mir Publ., 1978. 806 p.

23. Kim M.J., Flanagan W.F. The effect of plastic deformation on the resistivity and Hall Effect of copper-palladium and gold-palladium alloys. *Acta Metallurgica*, 1967, vol. 15, pp. 735–745. DOI: 10.1016/0001-6160(67)90354-9.

24. Garcia-Gonzalez M., Van Petegem S., Baluc N., Dupraz M., Honkimaki V., Lalire F., Van Swygenhoven H. Influence of thermo-mechanical history on the ordering kinetics in 18 carat Au alloys. *Acta Materialia*, 2020, vol. 191, pp. 186–197. DOI: 10.1016/j.actamat.2020.03.032.

25. Volkov A.Yu., Antonova O.V., Komkova D.A., Glukhov A.V., Volkova E.G., Livinets A.A., Podgorbunskaya P.O., Antonov B.D. Effect of moderate plastic deformation on structure and properties of the ordered Cu-56Au (at.%) alloy. *Materials Science and Engineering A*, 2023, vol. 865, p. 144626. DOI: 10.1016/j.msea.2023.144626.

26. Cahn R.W. Recovery, Strain-Age-Hardening and Recrystallization in Deformed Intermetallics. *High Temperature Aluminides and Intermetallics* / eds. Whang S.H. et al. The Minerals, Metals & Materials Society, 1990, p. 245–270.

27. Grinberg B.A., Ivanov M.A. *Intermetallidy Ni₃Al i TiAl: mikrostruktura, leformatsionnoe povedenie* [Intermetallics Ni3Al and TiAl: microstructure, deformation behavior]. Ekaterinburg, UrO RAN Publ., 2002. 359 p.

28. Volkov A.Yu., Podgorbunskaya P.O., Novikova O.S., Valiullin A.I., Glukhov A.V., Kruglikov N.A. Atomic ordering kinetics of Cu-56at.%Au alloy at a temperature of 250 °C. *Inorganic Materials*. 2023 (In print).

29. Grinberg B.A., Cyutkina V.I. *Novye metody uprochneniya uporyadochennykh splavov* [New methods for strengthening ordered alloys]. Moscow, Metallurgiya Publ., 1985. 175 p.

СПИСОК ЛИТЕРАТУРЫ

1. Kurnakov N., Zemczuzny S., Zasedatelev M. Transformations in Alloys of Gold with Copper // Journal of the Institute of Metals. 1916. Vol. 15. P. 305–331.

2. Jogansson C.H., Linde J.O. Röntgenographische und elektrische Untersuchungen der CuAu-Systems // Annalen der Physik. 1936. Vol. 417. № 1. P. 1–48. DOI: 10.1002/andp.19364170102.

3. Hirabayashi M. Stress-Ordering Effect on Thermal Expansion of CuAu Single Crystals // Journal of the Physical Society of Japan. 1959. Vol. 14. P. 149–152. DOI: 10.1143/JPSJ.14.149.

4. Van Tendeloo G., Amelinckx S., Jeng S.J., Wayman C.M. The initial stages of ordering in CuAuI and CuAuII // Journal of Materials Science. 1986. Vol. 21. P. 4395–4402. DOI: 10.1007/BF01106562.

5. Художественное литье из драгоценных металлов / под общ. ред. Л.А. Гутова. Л.: Машиностроение, 1988. 223 с.

6. Попова Л.А. Структурно-энергетические свойства бивакансий в сплаве CuAu I // Вестник Югорского государственного университета. 2022. Т. 66. № 3. С. 145–151. DOI: 10.18822/byusu202203145-151.

7. Larcher M., Cayron C., Blatter A., Soulignac R., Logé R.E. Electron backscatter diffraction study of variant selection during ordering phase transformation in $L1_0$-type red gold alloy // Journal of Applied Crystallography. 2019. Vol. 52. P. 1202–1213. DOI: 10.1107/S1600576719011890.

8. Федоров П.П., Волков С.Н. Фазовая диаграмма системы Au-Cu // Журнал неорганической химии. 2016. Т. 61. № 6. С. 809–812. DOI: 10.7868/S0044457X16060064.

9. Малышев В.М., Румянцев Д.В. Золото. М.: Металлургия, 1979. 288 с.

10. Trong D.N., Long V.C., Saraç U., Quoc V.D., Ţălu Ş. First-Principles Calculations of Crystallographic and Electronic Structural Properties of Au-Cu Alloys // Journal of Composites Science. 2022. Vol. 6. № 12. P. 383. DOI: https://doi.org/10.3390/jcs6120383.

11. Волков А.Ю., Казанцев В.А. Влияние исходного состояния на формирование структуры и свойств упорядоченного сплава CuAu // Физика металлов и металловедение. 2012. Т. 113. № 1. С. 66–76. DOI: 10.1134/S0031918X12010127.

12. Lamiri I., Martinez-Blanco D., Abdelbaky M.S.M., Mari D., Hamana D., García-Granda S. Investigation of the order-disorder phase transition series in AuCu by in-situ temperature XRD and mechanical spectroscopy // Journal of Alloys and Compounds. 2019. Vol. 770. P. 748–754. DOI: 10.1016/j.jallcom.2018.08.094.

13. Garcia-Gonzalez M., Van Petegem S., Baluc N., Hocine S., Dupraz M., Lalire F., Van Swygenhoven H. Enhanced precipitate growth at reduced temperatures during chemical ordering in deformed red gold alloys // Scripta Materialia. 2019. Vol. 170. P. 129–133. DOI: 10.1016/j.scriptamat.2019.05.038.

14. Volkov A.Yu., Antonova O.V., Glukhov A.V., Komkova D.A., Antonov B.D., Kostina A.E., Livinets A.A., Generalova K.N. Features of the disorder-order phase transition in non-stoichoimetric Cu-56at%Au alloy // Journal of Alloys and Compounds. 2022. Vol. 891. P. 161938. DOI: 10.1016/j.jallcom.2021.161938.

15. Farooq Z., Ali R., Ahmed N., Fahad M., Ahmad A., Yaseen M., Mahmood M.H.R., Hussain S., Rehan I., Zubair Khan M., Jan T., Qayyum M.A., Afzal M., Mahr M.S., Shafique M. Determination of the Gold Alloys Composition by Laser-Induced Plasma Spectroscopy Using an Algorithm for Matching Experimental and Calculated Values of Electron Number Density // Journal of Applied Spectroscopy. 2023. Vol. 90. P. 126–136. DOI: 10.1007/s10812-023-01513-x.

16. Gafner Y.Y., Gafner S.L., Golovenko Z.V. Analysis of the size distribution of binary Cu-Au nanoparticles during synthesis from a gaseous medium // Letters on Materials. 2020. Vol. 10. № 1. P. 33–37. DOI: 10.22226/2410-3535-2020-1-33-37.

17. Генералова К.Н., Глухов А.В., Волков А.Ю. Рентгеноструктурный анализ кинетики атомного упорядочения по типу $L1_0$ в нестехиометрическом медно-золотом сплаве // Вестник Пермского национального исследовательского политехнического университета. Машиностроение, материаловедение. 2018. Т. 20. № 2. С. 75–85. DOI: 10.15593/2224-9877/2018.2.09.

18. Volkov A.Yu., Novikova O.S., Antonov B.D. The kinetics of ordering in an equiatomic CuPd alloy: A resistometric study // Journal of Alloys and Compounds. 2013. Vol. 581. P. 625–631. DOI: 10.1016/j.jallcom.2013.07.132.

19. Glezer A.M., Timshin I.A., Shchetinin I.V., Gorshenkov M.V., Sundeev R.V., Ezhova A.G. Unusual behavior

of long-range ordered parameter in Fe₃Al superstructure under severe plastic deformation in Bridgman anvils // Journal of Alloys and Compounds. 2018. Vol. 744. P. 791–796. DOI: 10.1016/j.jallcom.2018.02.124.

20. Валиев Р.З., Александров И.В. Наноструктурные материалы, полученные интенсивной пластической деформацией. М.: Логос, 2000. 271 с.

21. Malis O., Ludwig K.F. Kinetics of phase transitions in equiatomic CuAu // Physical Review B. 1999. Vol. 60. № 21. P. 14675–14682. DOI: 10.1103/PhysRevB.60.14675.

22. Кристиан Дж. Теория превращений в металлах и сплавах. Т. 1. М.: Мир, 1978. 806 с.

23. Kim M.J., Flanagan W.F. The effect of plastic deformation on the resistivity and Hall Effect of copper-palladium and gold-palladium alloys // Acta Metallurgica. 1967. Vol. 15. P. 735–745. DOI: 10.1016/0001-6160(67)90354-9.

24. Garcia-Gonzalez M., Van Petegem S., Baluc N., Dupraz M., Honkimaki V., Lalire F., Van Swygenhoven H. Influence of thermo-mechanical history on the ordering kinetics in 18 carat Au alloys // Acta Materialia. 2020. Vol. 191. P. 186–197. DOI: 10.1016/j.actamat.2020.03.032.

25. Volkov A.Yu., Antonova O.V., Komkova D.A., Glukhov A.V., Volkova E.G., Livinets A.A., Podgorbunskaya P.O., Antonov B.D. Effect of moderate plastic deformation on structure and properties of the ordered Cu-56Au (at.%) alloy // Materials Science and Engineering A. 2023. Vol. 865. P. 144626. DOI: 10.1016/j.msea.2023.144626.

26. Cahn R.W. Recovery, Strain-Age-Hardening and Recrystallization in Deformed Intermetallics // High Temperature Aluminides and Intermetallics / eds. Whang S.H. et al. Indianapolis: The Minerals, Metals & Materials Society, 1990. P. 245–270.

27. Гринберг Б.А., Иванов М.А. Интерметаллиды Ni₃Al и TiAl: микроструктура, деформационное поведение. Екатеринбург: УрО РАН, 2002. 359 с.

28. Волков А.Ю., Подгорбунская П.О., Новикова О.С., Валиуллин А.И., Глухов А.В., Кругликов Н.А. Кинетика атомного упорядочения сплава Cu-56ат.%Au при температуре 250 °C // Неорганические материалы. 2023 (в печати).

29. Гринберг Б.А., Сюткина В.И. Новые методы упрочнения упорядоченных сплавов. М.: Металлургия, 1985. 175 с.

Кинетика формирования сверхструктуры $L1_0$ в сплаве Cu–56Au (ат. %): резистометрическое исследование

© 2023

Подгорбунская Полина Олеговна*[*1,2], студент, лаборант лаборатории прочности*
Згибнев Дмитрий Александрович[1,2], *студент, лаборант лаборатории прочности*
Гаврилова Алена Антоновна[1,2], *студент, лаборант лаборатории прочности*
Новикова Оксана Сергеевна[2,3], *кандидат физико-математических наук,
старший научный сотрудник лаборатории прочности*
Волков Алексей Юрьевич[2,4], *доктор технических наук, заведующий лабораторией прочности*

[1]*Уральский федеральный университет имени первого Президента России Б.Н. Ельцина, Екатеринбург (Россия)*
[2]*Институт физики металлов имени М.Н. Михеева Уральского отделения РАН, Екатеринбург (Россия)*

***E-mail: podgorbunskaua@imp.uran.ru,
polina.podgorbunskaya@yandex.ru**

[3]ORCID: https://orcid.org/0000-0003-0474-8991
[4]ORCID: https://orcid.org/0000-0002-0636-6623

Аннотация: Благодаря повышенным прочностным свойствам в сравнении с эквиатомным сплавом Cu–50 ат. % Au, нестехиометрический сплав Cu–56 ат. % Au может найти применение не только в стоматологии, но и в качестве коррозионностойкого проводника слабых электрических сигналов для приборостроения. Работа посвящена изучению кинетики фазового превращения беспорядок→порядок в сплаве Cu–56Au, в ходе которого неупорядоченная ГЦК-решетка ($A1$-фаза) перестраивается в атомно-упорядоченную со сверхструктурой $L1_0$. Исходное разупорядоченное состояние сплава получали двумя способами: применением пластической деформации на 90 % или закалкой от температуры 600 °C (т. е. из области существования $A1$-фазы). Отжиги для формирования сверхструктуры $L1_0$ проводили при температурах 200, 225 и 250 °C. Продолжительность отжигов составляла от 1 ч до 2 мес. В качестве основной методики исследования кинетики превращения беспорядок→порядок была выбрана резистометрия. Получены температурные зависимости удельного электросопротивления сплава в различных структурных состояниях. Построены графики зависимости удельного электросопротивления от логарифма времени отжига, на основе которых проведена оценка скорости образования новой фазы. Для аттестации структурного состояния сплава на различных этапах превращения использовался рентгеноструктурный анализ (РСА). Перестройка кристаллической структуры в ходе превращения показана на примере расщепления пика (200) кубической исходной $A1$-фазы на два пика – (200) и (002) тетрагональной упорядоченной $L1_0$-фазы. По данным резистометрии и РСА проведена количественная оценка скорости фазового превращения беспорядок→порядок в исследуемом сплаве. Установлено, что значения доли превращенного объема (резистометрия) и степени дальнего

порядка (рентгеноструктурный анализ) близки. Показано, что в температурном интервале 200–250 °C скорость атомного упорядочения по типу $L1_0$ в нестехиометрическом сплаве Cu–56 ат. % Au максимальна при 250 °C. Установлено, что превращение беспорядок→порядок в исходно закаленных образцах исследованного сплава протекает приблизительно на порядок быстрее по сравнению с предварительно деформированными образцами.

Ключевые слова: Cu–56 ат. % Au; сплавы Cu–Au; атомное упорядочение; резистометрия; сверхструктурные рентгеновские отражения; оценка степени порядка.